

X-ray scattering as a probe for warm dense mixtures and high-pressure miscibility

K. Wünsch,¹ J. Vorberger,¹ G. Gregori,² and D.O. Gericke¹

¹*Centre for Fusion, Space and Astrophysics, Department of Physics,
University of Warwick, Coventry CV4 7AL, United Kingdom*

²*Clarendon Laboratory, University of Oxford, OX1 3PU, United Kingdom*
(Dated: May 24, 2010)

We demonstrate the abilities of elastic x-ray scattering to yield information on dense matter with multiple ion species and on the microscopic mixing in dense materials. Based on partial structure factors from *ab initio* simulations, a novel approach for the elastic scattering feature is applied to dense hydrogen-beryllium and hydrogen-helium mixtures. The scattering signal differs significantly between single species, real microscopic mixtures, and two separate fluids in the scattering volume.

PACS numbers: 52.27.Cm, 52.70.-m, 52.59.Hq

Most materials in nature and technical applications consist of multiple atomic species and their properties can be only understood if all mutual interactions are considered. This is also true for high energy density science applied to astrophysics and inertial confinement fusion. Indeed, objects such as old stars and giant gas planets can be considered as a natural laboratory for the equation of state of dense, high-pressure mixtures [1–4]. Demixing and the subsequent segregation of the heavy elements can play a crucial role in the energy balance of these objects [5]. Moreover, the assumed separation into helium-rich and helium-poor phases strongly influences the evolution and present internal structure of gas planets and might be the reason for the observed low helium concentration in the atmosphere and the high luminosity of Jupiter and Saturn. Phase separation in hydrogen-helium mixtures has been predicted by quantum simulation for conditions found in the interior of gas giants [6, 7]. However, the verification of these theoretical predictions in an astrophysical setting is quite indirect and requires full scale planet modeling where demixing or phase separation is one of many unknowns. Thus, laboratory experiments are needed to investigate these extreme conditions. This is even more true for such complex, but very interesting processes as the formation of pure carbon from methane under the high pressures found in Neptune [8].

Driven by the progress in inertial confinement fusion [9, 10], mixing receives currently also much interest in laboratory settings. As the boundary between the fuel and the ablator is hydrodynamically unstable during the compression phase, fuel and shell material (beryllium or carbon) mix. The degree of mixing strongly affects the performance of the target and can even prevent sufficient burn or ignition at all [11, 12]. However, experimental techniques to probe mixing under the extreme conditions in fusion targets prove to be very difficult and only a few spectroscopic investigations exist [13, 14]. These found however that present models for the mixing during the compression underestimate the experimental results.

In this Letter, we develop the theoretical framework for the application of elastic x-ray scattering as a tool

to investigate mixtures and the high-pressure miscibility of materials. X-ray Thomson scattering has been shown to robustly deliver basic plasma parameters like density, temperature, and ion charge state as well as dynamic and structural properties of simple materials [15–17]. First experiments with two-component systems like plastics (CH) or lithium hydrate (LiH) have been performed as well [18–21]. Hitherto the theoretical description of the spectrum was however based on an ion structure that was generated from a one-component calculation via [18]

$$S_{ab}(k) = \delta_{ab} + \frac{\sqrt{n_a n_b}}{n} \frac{Z_a Z_b}{\bar{Z}^2} \left[S_{ii}^{1C}(k) - 1 \right]. \quad (1)$$

Here, S_{ab} denote the partial structure factors. n_a and Z_a are the density and the charge of the ions of species a . The structure for the effective one-component system, i.e. S_{ii}^{1C} , is calculated using an average ion charge state defined by $\bar{Z} = \sum_a n_a Z_a / \sum_a n_a$. Such a treatment is only exact in the limit of weakly coupled plasmas that can be described by the random phase approximation (RPA) [22]. It is however unable to describe the highly nonlinear effects in the structure of strongly coupled ions [23]. Therefore, to apply x-ray scattering as a reliable diagnostic method for dense matter requires a theoretical description that considers the full microscopic structure in the materials tested including the nonlinear interplay between different highly correlated ion species. In contrast to the approach of Ref. [18], the new approach should also allow for Z -dependent screening clouds for different ion species.

Here, we derive a full multi-component description of the x-ray scattering signal. The partial structure factors required are obtained via density functional molecular dynamics simulations (details in Refs. [24, 25]). We show that the elastic scattering feature is very sensitive to the ratio of the different elements in the scattering volume. Thus, it can be used as a probe for the degree of mixing in strongly compressed samples. Moreover, we predict considerable differences in the scattering strength from microscopically mixed systems and matter consisting of two phases. The differences are particularly pronounced

for hydrogen-helium mixtures under conditions found in the interior of Jupiter. Thus, elastic x-ray scattering can be used to investigate demixing of hydrogen and helium under planetary conditions.

We briefly sketch our theoretical description of x-ray Thomson scattering that is developed along the ideas of Chihara [26, 27], but fully generalized to plasmas with multiple ion species. The influence of the ions is however quite indirect as x-rays are scattered by electron density fluctuations. The scattered intensity is thus proportional to the total electron structure factor $S_{ee}^{tot}(\mathbf{k}, \omega)$, where ω and k are the frequency and wave number shifts of the photon, respectively [28]. The structure factor can be expressed as the Fourier-transform of the intermediate scattering function with respect to time. The latter is the correlation function of electron densities

$$F_{ee}^{tot}(\mathbf{k}, t) = \langle \rho_e^{tot}(\mathbf{k}, t) \rho_e^{tot}(-\mathbf{k}, 0) \rangle. \quad (2)$$

Now we split the total electron density into free electrons and contributions of core electrons associated with N different ion species: $\rho_e^{tot}(\mathbf{k}, t) = \sum_a^N \rho_a^c(\mathbf{k}, t) + \rho^f(\mathbf{k}, t)$. Applying this decomposition in the quadratic form (2), we obtain N^2 bound-bound terms, N bound-free terms and one free-free term. All of these terms can be treated as in the case of just one ion species. Special care must be however given to core electrons belonging to different ions species $\sum_{a \neq b} \langle \rho_a^c(\mathbf{k}, t) \rho_b^c(-\mathbf{k}, 0) \rangle$ as it defines a distinct ion-ion scattering function without core excitations.

Evaluating the different density correlations, we obtain for the total electron structure factor (in the following, the k -dependence is dropped for simplicity)

$$\begin{aligned} S_{ee}^{tot}(\omega) &= \bar{Z} S_{ee}(\omega) + 2 \sum_a \sqrt{\bar{Z} x_a} f_a S_{ea}(\omega) \\ &+ \sum_a Z_a^c x_a \int d\omega' \tilde{S}_a^{ce}(\omega - \omega') S_a^S(\omega') \\ &+ \sum_{a,b} \sqrt{x_a x_b} f_a f_b S_{ab}(\omega). \end{aligned} \quad (3)$$

Here, we introduced the concentrations $x_a = n_a / \sum_a n_a$. Z_a^c is the number of core electrons bound to ions of the species a . The first term describes correlations between two free electrons. The next term accounts for free-bound correlations where f_a is the atomic/ionic form factor of bound states of component a . The second line contains self-contributions, i.e., internal excitations and bound-free transitions. Except the summation over species, it is unchanged from its usual form. The last term describes correlations between two bound electrons.

The main problem using the expression (3) is the fact that all partial structure factors are connected. This becomes particularly clear when considering S_{ee} which contains correlations between two screening clouds and, thus, also ionic properties. Indeed, the structure factors used in Eq. (3) form a set of $\frac{1}{2}N(N+1)$ equations [29].

This set can be conveniently written in matrix form and then inverted. Such a procedure yields

$$\bar{Z} S_{ea}(\omega) = x_a q_a S_{aa}(\omega) + \sum_{b \neq a} x_b q_b S_{ab}(\omega) \quad (4)$$

for the free-bound structure factor. Here, S_{ab} denotes the partial ion-ion structure factors. The correlations of the free electrons to the ions are contained in the screening function $q_a(k)$ which are defined via

$$q_a(k) = \frac{n_e C_{ea}(k) \chi_e^0(k)}{1 - n_e C_{ee}(k) \chi_e^0(k)}, \quad (5)$$

where C_{ee} and C_{ea} are the direct electron-electron and electron-ion correlation functions, respectively. In lowest order, these are given by the respective potentials. $\chi_e^0(k)$ denotes the density response of a free electron gas [29].

For the free-free structure factor, one obtains

$$\bar{Z} S_{ee}(\omega) = \sum_{a,b} \sqrt{x_a x_b} q_a q_b S_{ab}(\omega) + S_{ee}^0(\omega), \quad (6)$$

which now separates electron-ion correlations from the structure factor of the free electron gas $S_{ee}^0(k, \omega)$ that characterizes the kinetically free electrons in the system.

The results can be summarized in the total electron structure factor of the form

$$\begin{aligned} S_{ee}^{tot}(\omega) &= \sum_{a,b} \sqrt{x_a x_b} [f_a + q_a][f_b + q_b] S_{ab}(\omega) + \bar{Z} S_{ee}^0(\omega) \\ &+ \sum_a Z_a^c x_a \int d\omega' \tilde{S}_a^{ce}(\omega - \omega') S_a^S(\omega'). \end{aligned} \quad (7)$$

The first term describes quasi-elastic scattering at bound electrons and the screening clouds associated to different ion species. In this contribution, the full ionic structure, expressed by the partial structure factors S_{ab} , influences the scattering spectrum. As the ion motion cannot be resolved in current laser experiments, the ion structure can be treated statically: $S_{ab}(k, \omega) = S_{ab}(k) \times \delta(\omega)$. The static structure factors $S_{ab}(k)$ can be obtained by means of classical hypernetted chain (HNC) calculations [23] or numerical simulations [25, 30]. The second term contains the full dynamic response of the free electron gas which can be in lowest order described by the random phase approximation. Extensions include electron-ion collisions and local field corrections [31]. The last term describes contributions due to the excitation or ionization of bound electrons by x-rays.

The inelastic contributions due to scattering at free electrons, bound-free transitions, and internal excitations are unchanged from a description for systems with one ion species [18]. We thus concentrate here on elastic scattering, that is the first term of Eq. (7), which highlights the mutual correlations between the different ion species. To calculate the weight of the Rayleigh peak, i.e.,

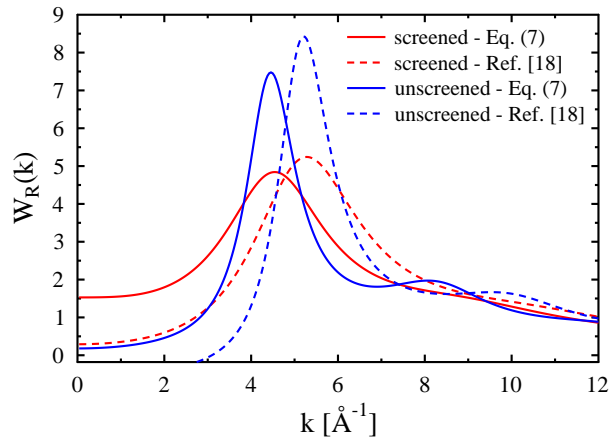


FIG. 1: Comparison of different treatments for the weight of the Rayleigh peak $W_R(k)$ (see text). Considered is a CH-plasma with $n_C = n_H = 2.3 \times 10^{23} \text{ cm}^{-3}$ and a temperature of $T = 1 \text{ eV}$. The ion charge states are $Z_C = 4$ and $Z_H = 1$. Both 1C and partial structure factors are calculated via HNC [23].

$W_R(k) = \sum_{a,b} \sqrt{x_a x_b} [f_a(k) + q_a(k)] [f_b(k) + q_b(k)] S_{ab}(k)$, we use structure factors from *ab initio* simulations (DFT-MD) [25] or solutions of the hypernetted chain equations (HNC) [23]. The screening functions are used in linear response to a Coulomb field, i.e., $q_a(k) = Z_a \kappa^2 / (\kappa^2 + k^2)$, where κ is the inverse electron screening length. The form factors f_a are taken from isolated atoms/ions [32].

First we compare the full multi-component formula (7) and the approximate treatment of Ref. [18] which is based on the structure of an average ion component via Eq. (1). Both approaches agree for weakly coupled systems, but large differences occur for strongly coupled systems as shown in Fig. 1 ($\Gamma_{ii} \approx 80$). For both the screened and unscreened ion systems, the maximum of the Rayleigh peak is shifted. This reflects the fact that the higher charged carbon ions imprint their structure into the proton subsystem which cannot be described by the one-component structure. Moreover, the mutual screening of the ions is neglected in the reduced model which results in a strongly underestimated Rayleigh peak at small k . The screened interactions are more realistic [17], but the results for unscreened ions demonstrate that the reduced model may even predict negative W_R (especially, for small k). For strongly coupled multi-component systems, the analysis should thus be based on the new expression (7).

Let us now turn to the application of the new multi-component description for the mixing of beryllium and hydrogen as it occurs during inertial fusion experiments. Due to the strong drive, the initially well-defined interface between the two materials experiences a Rayleigh-Taylor instability. At this stage, a volume element close to the original boundary will contain two fluids. However, these fluids consist of either pure beryllium or hydrogen and the system is made of two distinct phases. Later

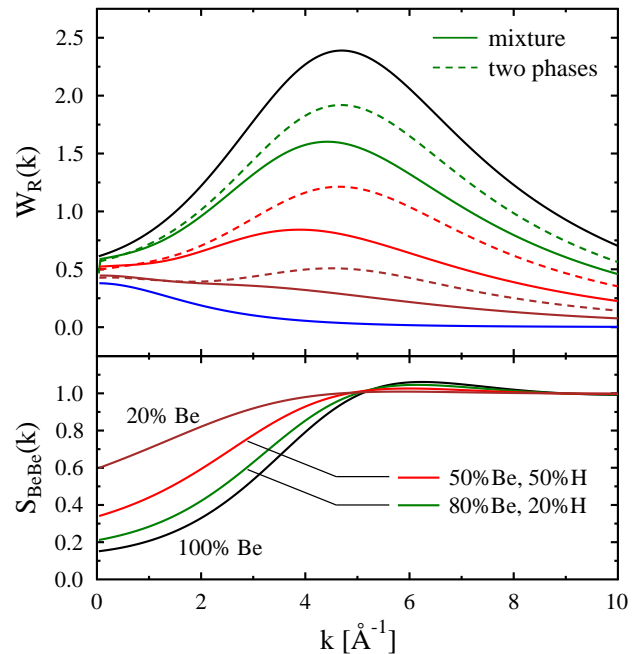


FIG. 2: (color online) The upper panel shows the weight of the Rayleigh peak, $W_R(k)$, for real microscopic mixtures of beryllium and hydrogen compared to systems that contain both materials in two pure phases. The concentrations of beryllium are (from top to bottom): 100%, 80%, 50%, 20%, and 0%. The temperature of the system is $T = 13 \text{ eV}$. The total densities were arranged to be in pressure equilibrium with pure beryllium at $n_{\text{Be}} = 3.707 \times 10^{23} \text{ cm}^{-3}$. The lower panel displays the partial beryllium-beryllium structure factor for the same concentrations.

both materials will microscopically mix due to diffusion.

Figure 2 demonstrates that the degree of mixing in dense beryllium-hydrogen systems can be investigated by measuring the strength of elastic x-ray scattering. To allow for experimental verification, we have taken the density and the temperature from a recent experiment on shocked pure beryllium [33]. Behind the shock front, all possible mixtures will be compressed until they are in pressure equilibrium with the driven beryllium. Thus, we have adjusted the total densities of the mixtures until the pressure matches the one of the pure beryllium. This procedure yields, e.g., a density of $n_H = 8 \times 10^{23} \text{ cm}^{-3}$ for the case of 100% hydrogen.

As beryllium scatters more efficiently than hydrogen, the elastic feature is a strong function of the mixing ratio. Interestingly, both microscopic mixtures and two-phase systems scatter very similar at small k . Here, the signal is mainly determined by the partial beryllium-beryllium structure factor and we can use these data to determine the concentrations. However, significant differences arise at the maximum of the elastic scattering peak around $k = 5 \text{ Å}^{-1}$ that can be used to distinguish between hydrodynamic and diffusive mixing.

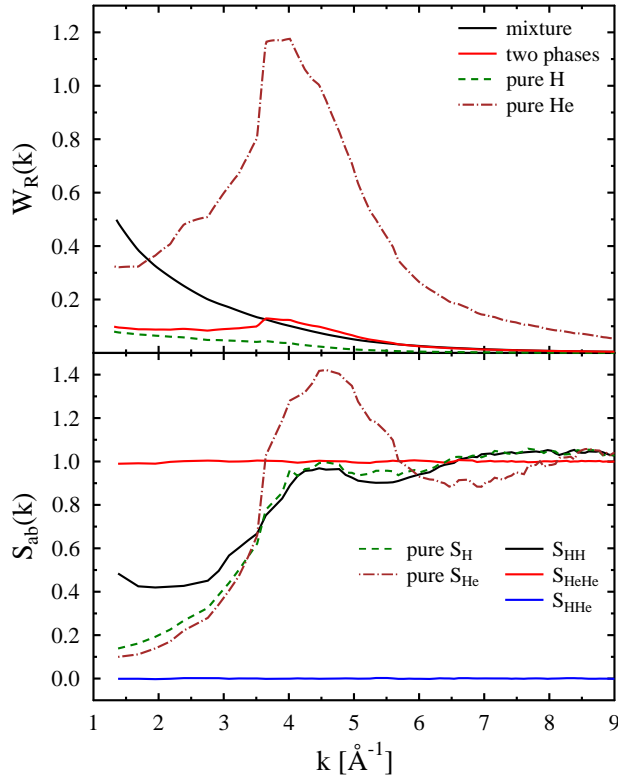


FIG. 3: (color online) Strength of the elastic scattering peak for pure hydrogen, pure helium, and a mixture with $x_H = 0.924$ and $x_{He} = 0.076$ at a temperature of $T = 5000$ K (upper panel). All systems have an electron density of $n_e = 4.7 \times 10^{23} \text{ cm}^{-3}$. The lower panel shows the partial structure factors of the three systems above.

In the next example, we investigate a hydrogen-helium mixture under conditions as found in the interior of giant gas planets [$x_{He} = n_{He}/(n_{He} + n_H) = 0.0756$]. Density and temperature yield a system in the atomic/molecular phase (no ionization). Fig. 3 shows that the strength of the elastic scattering feature displays large differences between the pure substances and the mixture. Indeed, we find very distinct scattering features for the different systems: pure helium scatters by far the most effectively and displays a peak around $k = 4 \text{ \AA}^{-1}$, the mixture shows a monotonically decreasing shape, and $W_R(k)$ for pure hydrogen is almost featureless. Due to the mixing ratio, the two phase system is dominated by the properties of hydrogen.

The reason for this behavior lies not only in the fact that helium atoms scatter the x-rays more efficiently. The different structure factors play also an important role. These structure factors were calculated from *ab initio* quantum simulations (see Ref. [24]) which allows us to treat neutral systems as well. Pure helium has a strong peak in the structure factor which is also clearly visible in the elastic scattering peak. This feature disappears in the mixture as the helium concentration is low. However, the

small fraction of helium mitigates the correlations within the hydrogen subsystem. Thus, small hydrogen-helium correlations lead to a shape of W_R that is dominated by the decreasing atomic form factor. Similar results are also found for denser and hotter systems where hydrogen and helium are ionized (not shown).

In conclusion, we have derived a novel description for x-ray scattering in systems with multiple atomic or ion species that take all the mutual correlations into account. The results show that x-ray scattering is a powerful tool to investigate dense mixtures and the mixing/demixing of materials under extreme conditions as they are found during inertial confinement fusion and in the interior of old stars and giant planets.

We acknowledge financial support from EPSRC (via grants EP/D062837 and EP/G007187/1) and STFC.

-
- [1] P. Dufour *et al.*, *Nature* **450**, 522 (2007).
 - [2] B. Militzer *et al.*, *Astrophys. J. Lett.* **688**, L45 (2008).
 - [3] N. Nettelmann *et al.*, *Astrophys. J.* **683**, 1217 (2008).
 - [4] J. Daligault and S. Gupta, *Astrophys. J.* **703**, 994 (2009).
 - [5] T. Guillot, *Science* **286**, 72 (1999).
 - [6] W. Lorenzen *et al.*, *Phys. Rev. Lett.* **102**, 115701 (2009).
 - [7] H.F. Wilson and B. Militzer, *Phys. Rev. Lett.* **104**, 121101 (2010).
 - [8] F. Ancilotto *et al.*, *Science* **275**, 1288 (1997).
 - [9] S.H. Glenzer *et al.*, *Science* **327**, 1228 (2010).
 - [10] C.K. Li *et al.*, *Science* **327**, 1231 (2010).
 - [11] J. Lindl, *Phys. Plasmas* **2**, 3933 (1995).
 - [12] S. Atzeni and J. Meyer-ter-Vehn *The Physics of Inertial Fusion* (Clarendon Press, Oxford, 2004).
 - [13] L. Welser-Sherrill *et al.*, *Phys. Rev. E* **76**, 056403 (2007).
 - [14] L. Welser-Sherrill *et al.*, *High Energy Density Physics* **5**, 249 (2009).
 - [15] S.H. Glenzer *et al.*, *Phys. Rev. Lett.* **90**, 175002 (2003).
 - [16] S.H. Glenzer *et al.*, *Phys. Rev. Lett.* **98**, 065002 (2007).
 - [17] E. Garcia Saiz *et al.*, *Nature Phys.* **4**, 940 (2008).
 - [18] G. Gregori *et al.*, *JQSRT* **99**, 225 (2006).
 - [19] H. Sagawa *et al.*, *Phys. Plasmas* **14**, 122703 (2007).
 - [20] A.L. Kritcher *et al.*, *Science* **322**, 69 (2008).
 - [21] B. Barbrel *et al.*, *Phys. Rev. Lett.* **102**, 165004 (2009).
 - [22] H. Totsuji, *Phys. Rev. A* **24**, 1077 (1981).
 - [23] K. Wünsch *et al.*, *Phys. Rev. E* **77**, 056404 (2008).
 - [24] J. Vorberger *et al.*, *Phys. Rev. B* **75**, 024206 (2007).
 - [25] K. Wünsch *et al.*, *Phys. Rev. E* **79**, 010201(R) (2009).
 - [26] J. Chihara, *J. Phys. F: Met. Phys.* **17**, 295 (1987).
 - [27] J. Chihara, *J. Phys.: Condens. Matter* **12**, 231 (2000).
 - [28] S.H. Glenzer and R. Redmer, *Rev. Mod. Phys.* **81**, 1625 (2009).
 - [29] D. Kremp, M. Schlages, and W.-D. Kraeft, *Quantum Statistics of Nonideal Plasmas* (Springer, Berlin, 2006).
 - [30] J.P. Hansen and I.R. McDonald, *Theory of Simple Liquids* (Academic Press, London, 1990).
 - [31] C. Fortmann *et al.*, *Phys. Rev. E* **81**, 026405 (2010).
 - [32] M.W.C. Dharma-wardana and F. Perrot, *Phys. Rev. A* **45**, 5883 (1992).
 - [33] H.J. Lee *et al.*, *Phys. Rev. Lett.* **102**, 115001 (2009).